

# Linear growth of entanglement entropy in holographic thermalization captured by horizon interiors and mutual information

Yong-Zhuang Li<sup>1</sup>, Shao-Feng Wu<sup>1,2\*</sup>, Yong-Qiang Wang<sup>3</sup>, and Guo-Hong Yang<sup>1,2</sup>

<sup>1</sup>*Department of physics, Shanghai University, Shanghai, 200444, P. R. China*

<sup>2</sup>*The Shanghai Key Lab of Astrophysics,  
Shanghai, 200234, P. R. China and*

<sup>3</sup>*Institute of Theoretical Physics, Lanzhou University, Lanzhou, 730000, P. R. China*

## Abstract

We study the holographic entanglement entropy in a homogeneous falling shell background, which is dual to the strongly coupled field theory following a global quench. For  $d=2$  conformal field theories, it is known that the entropy has a linear growth regime if the scale of the entangling region is large. In addition, the growth rate approaches a constant when the scale increases. We demonstrate analytically that this behavior is directly related to the part of minimal area surface probing the interior of apparent horizons in the bulk, as well as the mutual information between two disjoint rectangular subsystems in the boundary. Furthermore, we show numerically that all the results are universal for the  $d=3$  conformal field theory, the non-relativistic scale-invariant theory and the dual theory of Gauss-Bonnet gravity.

PACS numbers: 11.25.Tq, 12.38.Mh, 11.25.Tq, 03.65.Ud

---

\* Corresponding author. Email: sfwu@shu.edu.cn; Phone: +86-021-66136202.

## I. INTRODUCTION

As the most concrete realization of holographic principle, the gauge/gravity duality [1] has been fruitful in revealing universal features of strongly coupled field theories by gravitational description and also has the potential ability of encoding the quantum gravity using field theory language.

The duality has gone beyond the equilibrium and near-equilibrium processes, relating the thermalization of far-from-equilibrium boundary gauge theories to the gravitational collapse and the formation of black holes in the bulk. The non-equilibrium holography is well motivated by the demand of describing the fast thermalization of the quark gluon plasma produced in heavy ion collisions at the Relativistic Heavy Ion Collider [2], in which the onset of a hydrodynamic regime is found to be earlier than weak coupling estimates [3], and of describing the quantum quench that indicates the unitary evolution of a quantum system with a sudden change of coupling constants and can be realized experimentally in cold atom systems [4].

In order to explore the dynamics and the scale dependence of thermalization processes, the local observables, such as the expectation values of energy-momentum tensor, can not provide sufficient information as in the situation of viscous hydrodynamics. One important non-local observable is the entanglement entropy (EE) between some spatial region and its complement [5]. Usually EE is taken as a valuable probe to assess the amount of entanglement and acts as an order parameter to witness various quantum phases [6]. Moreover, EE does not depend on the details of theories and exists even in non-equilibrium quantum systems in which there is no well-defined thermal entropy and temperature.

A precise holographic description of EE has been proposed via AdS/CFT correspondence [7]. It is calculated as the area of the minimum surface in the bulk with its UV boundary coincident with the entangling surface in the dual field theory. The prescription of holographic entanglement entropy (HEE) has passed many nontrivial tests [8], but there is no formal derivation until very recently [9]. Respecting the clear geometric image of HEE and the important role of quantum entanglement in many-body quantum systems, the comparison between HEE and EE may be very useful to provide new insights into the quantum structure of spacetime [10–19], particularly in the framework of the entanglement renormalization [20]. Although HEE is previously defined only for static systems, a covariant generalization

is applicable to dynamical cases [21], where one should calculate HEE as the area of extremal surface and select the minimum one if there are several extremal surfaces.

There is another interesting non-local observable, namely the mutual information (MI) [5], which measures the total (both classical and quantum) correlations between two spatial subregions and acts as an upper bound of the connected correlation functions in those regions [22]. MI is related to EE closely. Considering two subsystems  $A$  and  $B$ , one can define MI as  $I(A, B) = S_A + S_B - S_{A \cup B}$ , where  $S_A$  denotes the EE on the subregion  $A$ . MI shares many features of EE in nontrivial ways. For instance, EE has a ubiquitous area law, that is divergent due to the presence of high energy singularities in unregulated quantum field theories. The divergent contributions cancel in MI between separate regions, leaving it as a scheme-independent quantity. But when  $A$  and  $B$  approach each other, the same short-distance divergence of EE appears again [23]. It has been found in CFTs that MI has power to extract more refined information than EE [24]. MI has also been studied in strongly coupling field theories with gravity duals both in static [15, 23, 25–27] and dynamic background [28–30]. In particular, for  $l \gg \beta$  where  $l$  is the size of  $A$  and  $\beta$  is the inverse temperature, it was found [31] that the static HEE (both for  $d$ -dim relativistic CFTs and non-relativistic scale-invariant theories) can be schematically decomposed as  $S_A = S_{div} + S_{thermal} + S_{finite} + S_{corr}$ , where  $S_{div}$  is the divergent boundary law,  $S_{thermal}$  is thermal entropy,  $S_{finite}$  follows an area law and  $S_{corr}$  is the correction suppressed by exponentials of  $l$ . Accordingly, for  $l \gg \beta$  and  $x \ll \beta$  (where  $x$  is the size of the separation between two same subregions  $A$  and  $B$ ), the holographic mutual information (HMI) can be decomposed as  $I = I_{div} + S_{finite} + I_{corr}$ , where  $I_{div} = S_{div}$  appears in the limit of  $x \rightarrow 0$  and  $I_{corr}$  are correction terms suppressed by exponentials of  $l$  and powers of  $x$  [32]. Obviously, the decomposition reveals that HMI can capture some important information of HEE[64].

In this paper, we will investigate the entanglement entropy in the thermalization process of the strongly coupled field theory following a global quench. The holographic thermalization related to the global quench have been discussed in [13, 33–41]. We will adapt the simple Vaidya model [13, 35–41], which describes a homogeneous falling thin shell of null dust and is a good quantitative approximation of the background generated by the perturbation of a time-dependent scalar field [33] and of the model of Ref. [42]. Among many interesting properties of holographic thermalization that have been found in term of the Vaidya model, it was observed that the evolution of HEE includes an intermediate stage during which it

is a simple linear function of time. The linear regime is not obvious when  $l$  is small, but it will be when  $l$  increases. This result matches well with the behavior seen in  $d=2$  CFTs [43, 44]. Also it is consistent with the evolution of coarse-grained entropy in nonlinear dynamical systems. There, it has been known that the linear growth rate of coarse-grained entropy is generally described by the Kolmogorov-Sinai entropy rate [45]. In classical 4-dim  $SU(2)$  lattice gauge theory, the Kolmogorov-Sinai entropy rate is shown to be an extensive quantity [46]. For strongly coupled field theory with gravity dual, it has been found [38] that the growth rate of HEE density in  $d=2$  CFTs is also nearly volume-independent for small boundary volumes. For large volumes, however, the growth rate of HEE approaches a constant limit [65].

One of the main motivations of this paper is to ask: whether the linear time growth of HEE with a volume-independent rate is the dynamical correspondence of the sub-leading area law of HEE captured by HMI in the static background? More simply, can the dynamical HMI capture the constant growth rate? To answer this question, we address the following work.

At first, we analytically prove that it is true for  $d=2$  CFTs. Then we check it using semi-analytic methods [66]. Furthermore, by implementing a time-consuming numerical computation, we can obtain the HEE with the large enough volume to demonstrate the constant growth rate of dynamical HEE in the  $d=3$  relativistic CFT, the  $d=3$  non-relativistic scale-invariant theory and the dual theory of 5-dimensional (-dim) Gauss-Bonnet (GB) gravity. Also, the linear growth with a constant slope is shown in the time evolution of HMI. It deserves to note that we need to find a Vaidya metric in asymptotically Lifshitz spacetime for studying the non-relativistic theory and the formula of HEE of GB gravity has the nontrivial correction (not same as the Wald entropy) to the one of Einstein gravity [47–50].

On the other hand, it is well known that the interior of black holes is difficult to probe. So it is impressed that the holographic calculation of dynamical non-local observables involves the information behind the apparent horizon generated in the process of gravitational collapse [28, 29, 35–38, 51–53]. Recently, Hartman and Maldacena further isolated the origin of the linear growth of HEE as arising from the growth of black hole interior measured along a special critical spatial slice [19]. Their result was obtained by studying the CFTs with the initial states of thermofield double for thermal states and a particular pure state, which are dual to eternal black holes and the eternal black holes with an end of the world brane that

cuts them in half, respectively.

Motivated by the insight that relating the horizon interior to the linear growth of HEE, the second aim of this paper is to study whether the interior of the apparent horizon along the extremal surface is also responsible for the linear growth of HEE in Vaidya models[67]. We demonstrate that the answer is affirmative at large  $l$  in various holographic theories. Thus we can present a very general result that in the process of holographic thermalization, the linear growth with a constant rate of EE can be captured by MI in the boundary and the horizon interior in the bulk.

The rest of the paper is arranged as follows. In Sec. II, we demonstrate that the HEE has a linear growth regime when  $l$  is large and the growth rate approaches a constant limit when  $l$  increases. In Sec. III, the evolution of HMI is shown to contain the regime of the linear growth with the constant rate. In Sec. IV, it is revealed that the extremal surfaces probing the interior of apparent horizons account for the linear growth of HEE at large  $l$ . In each section, we study the  $d=2$ ,  $d=3$  relativistic CFTs, the  $d=3$  non-relativistic scale-invariant theory and the dual theory of 5-dim GB gravity, respectively. For  $d=2$ , we will use analytic and semi-analytic methods. For other cases, only the numerical method is applicable. The conclusion and discussion are given in Sec. V. We also add three appendix. One is to look for a Vaidya metric in asymptotically Lifshitz spacetimes. The second is to extend the decomposition of static HEE and HMI in Refs. [31, 32] to the case of GB gravity by numerical fitting. At last appendix, we study the extremal surface in the interior of event horizon.

## II. LINEAR GROWTH OF HEE

At the beginning, let us set a general frame that can accommodate all our interested holographic theories as special cases. We will study the thermalization processes of  $d$ -dim strongly coupled field theories modeled by a homogeneous falling thin shell of null dust in  $(d+1)$ -dim spacetime. Consider such a spacetime in the Poincaré coordinates

$$ds^2 = -\frac{1}{z^{2n}}f_1(z,v)dv^2 - \frac{2}{z^2}f_2(z)dzdv + \frac{1}{z^2L_c^2}d\vec{x}^2. \quad (1)$$

Here  $z$  is the inverse of radial coordinate  $r$ . The spatial boundary coordinates are denoted as  $\vec{x} = (x_1, \dots, x_{d-1})$  and the translational invariance along  $\vec{x}$  directions characterizes the

global quench in the boundary theory. In addition,  $v$  labels the ingoing null coordinate and we take the shell falling along  $v = 0$ . The dynamical exponent  $n$  reflects the scale invariance and the effective curvature radius of space can be given by  $L_c^2 = 1/f_1(z, v)|_{z \rightarrow 0}$ . For three kinds of holographic theories that we are interested in [68], the unspecified quantities in the metric are different but they are all restricted to be a Vaidya spacetime with a massless shell. In addition, we will be interested in the case where the shell is infalling and intermediates the vacuum and black brane.

For  $d$ -dim CFTs, the desired AdS-Vaidya collapse geometry has been specified in [35, 38] with

$$f_1(z, v) = 1 - m(v)z^d, \quad f_2(z) = 1, \quad n = 1, \quad L_c = 1. \quad (2)$$

Note that we set AdS radius as 1. The mass function of the shell is

$$m(v) = \frac{M}{2} \left[ 1 + \tanh \frac{v}{v_0} \right],$$

where  $M$  denotes the mass for  $v > v_0$  and  $v_0$  represents a finite shell thickness. We will be interested in the zero thickness limit, which means to set the energy deposition on the boundary as instantaneous. Since the general Vaidya metric for GB gravity has been found in [54], the asymptotically AdS geometry with null collapse is easily obtained by requiring

$$f_1(z, v) = \frac{1}{2\alpha} \left\{ 1 - \sqrt{1 - 4\alpha [1 - m(v)z^d]} \right\}, \quad f_2(z) = 1, \quad n = 1, \quad L_c = \sqrt{\frac{1 + \sqrt{1 - 4\alpha}}{2}}, \quad (3)$$

where  $\alpha$  is the GB coupling constant. We also have interested in studying the holographic thermalization of a 3-dim non-relativistic field theory dual to a simple Lifshitz gravity [55], for which the static HMI has been studied in [32]. So we construct an asymptotical Lifshitz geometry with null collapse in Appendix A, which gives [69]

$$f_1(z, v) = 1 - m(v)z^2, \quad f_2(z) = z^{1-n}, \quad n = 2, \quad L_c = 1. \quad (4)$$

We will use HEE to probe the thermalization process. According to Ryu and Takayanagi's proposition, the EE of a spatial region  $A$  in a  $d$ -dim strongly coupled field theory has a dual gravitational description, which can be given by

$$S = \frac{1}{4G_N^{d+1}} \int_{\Sigma} dx^{d-1} \sqrt{h}, \quad (5)$$

where  $G_N^{d+1}$  is the  $(d+1)$ -dim gravitational constant and  $h$  corresponds to the determinant of the induced metric of the minimal surface  $\Sigma$ , which extends into the bulk and shares the

boundary with  $\partial A$ . In dynamical cases, one should calculate HEE as the area of extremal surface and select the minimal one if there are several extremal surfaces. The prescription of Eq. (5) has been used in non-relativistic theories [39, 56]. But for GB gravity, it has been presented that Eq. (5) should be modified as [47–49]

$$S = \frac{1}{4G_N^{d+1}} \left\{ \int_{\Sigma} dx^{d-1} \sqrt{h} \left[ 1 + \frac{2\alpha}{(d-2)(d-3)} \mathcal{R}_{\Sigma} \right] + \frac{4\alpha}{(d-2)(d-3)} \int_{\partial\Sigma} dx^{d-2} \sqrt{\sigma} \mathcal{K} \right\} \quad (6)$$

where  $\mathcal{R}_{\Sigma}$  is the induced scalar curvature of surface  $\Sigma$ ,  $\sigma$  is the determinant of the induced metric of the boundary  $\partial\Sigma$ , and  $\mathcal{K}$  is the trace of the extrinsic curvature of  $\partial\Sigma$ . Eq. (6) should be extremized and the minimal one should be selected as the definition of the HEE. Note that the last term is the Gibbs-Hawking term that ensures a good variational principle in extremizing the functional.

To fix the extremal surface, we need to specify the boundary region. In this paper, we are interested in a rectangular boundary region with one dimension of length  $l$  and the other  $d-2$  dimensions of volume  $R^{d-2}$ . We assume that the rectangular strip is translationally invariant except along the  $x_1$  direction. We also assume that  $l$  is along  $x_1$  direction and denote  $y = x_1$  for convenience.

In general, the extremal surfaces can be derived by extremizing Eq. (5) or Eq. (6). Substituting the Vaidya metric (1) into them, HEE can be described as

$$S = \frac{R^{d-2}}{4G_N^{d+1}} \int dy \frac{1}{z^{d-2}} \sqrt{z^{-2} - z^{-2n} f_1 v'^2 - 2z^{-2} f_2 z' v'} \quad (7)$$

for CFTs and Lifshitz gravity where  $' \equiv d/dy$ , or

$$S = \frac{R^{d-2}}{4G_N^{d+1}} \int \frac{dy}{d-2} \frac{z^2}{(zL_c)^{d+1}} L_c^3 \Phi \left\{ (d-2) + 2\alpha \left[ (d-4)z^2 L_c^2 + (d-2) \frac{z'^2}{\Phi^2} \right] \right\} \quad (8)$$

for GB gravity with  $\Phi = \sqrt{\frac{1}{L_c^2} - f_1 v'^2 - 2z' v'}$ . Extremizing Eq. (7), one can derive the two equations of motions

$$\begin{aligned} z'' = \frac{z^{-4n}}{2f_2^2} \{ & z^3 v'^2 f_1 [2(d+n-2)f_1 - z\partial_z f_1] - z^{2+2n} v' f_2 (v'\partial_v f_1 + 2z'\partial_z f_1) \\ & + 2z^{1+2n} f_1 [1-d+2(d+n-2)v'z'f_2] - 2z^{4n} z'^2 f_2 \partial_z f_2 \}, \end{aligned} \quad (9)$$

$$v'' = \frac{1}{2zf_2} \{ 2(d-1)(1-2v'z'f_2) + z^{2-2n} v'^2 [z\partial_z f_1 - 2(d+n-2)f_1] \}. \quad (10)$$

We will not write clearly the cumbersome equations of motions from Eq. (8).

To solve the equations of motion, one needs to fix the boundary conditions. We set the two sides of the rectangular strip as  $y = \pm \frac{l}{2}$  and set boundary time  $t_0 = 0$  when the shell just leaves the boundary. In summary, the boundary conditions are

$$z(\pm \frac{l}{2}) = z_0, \quad v(\pm \frac{l}{2}) = t_0, \quad (11)$$

where  $z_0$  is the cut-off close to the boundary. In addition, respecting the symmetry of extremal surfaces in our setting, we have

$$z'(0) = 0, \quad v'(0) = 0. \quad (12)$$

Using these boundary conditions, one can try to solve the equations of motions and obtain the HEE in terms of Eq. (7) and Eq. (8). However, the equations of motions are difficult to be solved analytically in general.

At late time, the HEE  $S$  will approach the equilibrium value  $S_{thermal}$ . It can be obtained by Eq. (7) and Eq. (8) in the background of pure black branes where the mass function  $m(v)$  in  $f_1$  should be replaced with the mass parameter  $M$ . Thus, one can obtain the conservation equations

$$1 - z^{2-2n} f_1(z) v'^2 - 2f_2(z) z' v' = \left( \frac{z_*}{z} \right)^{2(d-1)} \quad (13)$$

for CFTs and Lifshitz gravity, and

$$\frac{1}{L_c} \left( \frac{z_*}{z} \right)^{d-1} \left\{ 1 - \frac{2(d-2) z'^2 L_c^4 \alpha}{[d-2 + 2(d-4) z_*^2 \alpha] \Phi_1^2} \right\} = \Phi_1,$$

for GB gravity, where  $z_* = z(0)$  and  $\Phi_1 = \sqrt{\frac{1}{L_c^2} - f_1(z) v'^2 - 2z' v'}$ . In terms of the two conservation equations and the coordinate transformation  $dv = dt - z^{n-1} dz / f_1$ , the static HEE can be obtained. For CFTs and Lifshitz gravity, it is given by

$$S_{thermal} = \frac{R^{d-2}}{2G_N^{d+1}} \int_{z_0}^{z_*} \frac{dz}{z^{d+2n-3}} \sqrt{\frac{2z^{3n-3} f_2(z) - 1}{f_1(z) [1 - (z/z_*)^{2(d-1)}]}} \quad (14)$$

For GB gravity, the result is cumbersome and is not presented here clearly.

### A. d=2 CFTs

In Ref. [38], Balasubramanian et al. present an analytical method to compute the length of geodesic in the  $AdS_3$ -Vaidya spacetime dual to d=2 CFTs. The basic idea of this method



is to separate the geodesic into the part inside the shell and the part outside. The inside is described by the pure AdS metric and the outside by the static BTZ black brane geometry. Minimizing the total length of two parts of the geodesic, one can fix the geodesic that is anchored at two sides of the rectangular strip on the boundary and chases the shell falling along  $v = 0$ . Let us review this method briefly.

Outside the shell, the spacetime metric is

$$ds^2 = -(r^2 - r_H^2)dt^2 + \frac{dt^2}{r^2 - r_H^2} + r^2 dx^2 \text{ with } t = v - \frac{1}{2r_H} \log \left| \frac{r - r_H}{r + r_H} \right|,$$

where  $r_H$  is the location of horizon. The spatial geodesic is determined by

$$\lambda_{\pm}^{out} = \frac{1}{2} \ln \left[ -1 + E^2 - J^2 + \frac{2r^2}{r_H^2} \pm \frac{2}{r_H^2} \sqrt{D(r)} \right], \quad (15)$$

$$t_{\pm}^{out} = t_0 + \frac{1}{2r_H} \ln \left| \frac{r^2 - (E+1)r_H^2 \pm \sqrt{D(r)}}{r^2 + (E-1)r_H^2 \pm \sqrt{D(r)}} \right|,$$

$$x_{\pm}^{out} = \frac{1}{2r_H} \ln \left[ \frac{r^2 - Jr_H^2 \pm \sqrt{D(r)}}{r^2 + Jr_H^2 \pm \sqrt{D(r)}} \right], \quad (16)$$

$$v_{\pm}^{out} = t_0 + \frac{1}{2r_H} \ln \left[ \frac{r - r_H}{r + r_H} \frac{r^2 - (E+1)r_H^2 \pm \sqrt{D(r)}}{r^2 + (E-1)r_H^2 \pm \sqrt{D(r)}} \right], \quad (17)$$

$$D(r) = r^4 + (-1 + E^2 - J^2)r_H^2 r^2 + J^2 r_H^4,$$

where  $E$  and  $J$  are conserved charges concerning energy and angular momentum, respectively. The subscript “+” denotes branch 1 and “−” means branch 2. Both of them are necessary to give the complete geodesic in general. The superscript “out” denotes the part of the geodesic outside the shell. The part inside the shell, that is denoted by the superscript “in”, can be described similarly by

$$\lambda_{\pm}^{in} = \pm \cosh^{-1} \left( \frac{r}{r_*} \right), \quad (18)$$

$$t^{in} = \frac{1}{r_{sw}} = \text{const.},$$

$$x_{\pm}^{in} = \pm \frac{1}{r_*} \sqrt{1 - \left( \frac{r_*}{r} \right)^2}, \quad (19)$$

$$v^{in} = \frac{1}{r_{sw}} - \frac{1}{r}, \quad (20)$$

where  $r_*$  denotes the radial endpoint of the geodesic inside the shell and  $r_{sw}$  is the radial location at which the geodesic intersects the shell. Here “ $\pm$ ” denote that the part of geodesic in pure AdS region is symmetric. Extremizing the total geodesic length, one can obtain the

refraction conditions, which give out the conserved charges of the outside geodesic. For branch 1 with  $r_{sw} \geq r_H/\sqrt{2}$  and branch 2 with  $r_{sw} \leq r_H/\sqrt{2}$ , the conserved charges are

$$E = -\frac{r_H \sqrt{r_{sw}^2 - r_*^2}}{2r_{sw}^2}, \quad J = +\frac{r_*}{r_H}, \quad (21)$$

where we have selected the proper sign combination to ensure a finite  $v$  when the geodesic crosses the future horizon. With the mind that the shell is falling along  $v = 0$  and the spatial separation on the boundary is fixed as  $l$ , one can obtain the parameters  $r_{sw}$  and  $r_*$  from

$$2\rho = \coth(r_H t_0) + \sqrt{\coth^2(r_H t_0) - \frac{2c}{c+1}} \quad (22)$$

$$l = \frac{1}{r_H} \left\{ \frac{2c}{s\rho} + \ln \left[ \frac{2(1+c)\rho^2 + 2s\rho - c}{2(1+c)\rho^2 - 2s\rho - c} \right] \right\}, \quad (23)$$

where

$$\rho = r_{sw}/r_H, \quad \rho s = r_*/r_H, \quad s = \sqrt{1 - c^2}. \quad (24)$$

Finally, the sum of the length of inside and outside geodesics can be written as

$$L(l, t_0) = 2 [\lambda_+^{in}(r_{sw}) - \lambda_+^{in}(r_*)] + 2 [\lambda_+^{out}(r_0) - \lambda_-^{out}(r_{sw})] \quad (25)$$

$$= 2 \ln \left[ \frac{2r_0 \sinh(r_H t_0)}{r_H s(l, t_0)} \right], \quad (26)$$

where  $r_0 = 1/z_0$  denotes a UV cutoff and  $s(l, t_0)$  is an implicit function determined by Eqs. (22), (23) and (24). In Eq. (25), it seems that we have assumed the branch 2 intermediates the branch 1 and the inside geodesic. However, the result is same for another case in which the branch 1 connects the inside geodesic directly. This is because  $\lambda_+^{out}(r_{sw})$  with  $r_{sw} \geq r_H/\sqrt{2}$  has the same form as  $\lambda_-^{out}(r_{sw})$  with  $r_{sw} \leq r_H/\sqrt{2}$ .

Although the geodesic has been described by analytical formula, the implicit function  $s(l, t_0)$  in Eq. (26) can be solved only by numerical methods in general. This is why we call this method as the semi-analytical method. Fortunately, the analytical expansion of Eq. (26) has been found in the large boundary region [36] or in the period of the early time growth and late time saturation [13]. They are even applicable to calculate the non-equal time two-point functions and allow for the different geometry inside the shell. Here we will give a simplified version of the analytical method which is enough for giving an analytical solution in the region that we have interested in, namely, the large  $lr_H$  and intermediate

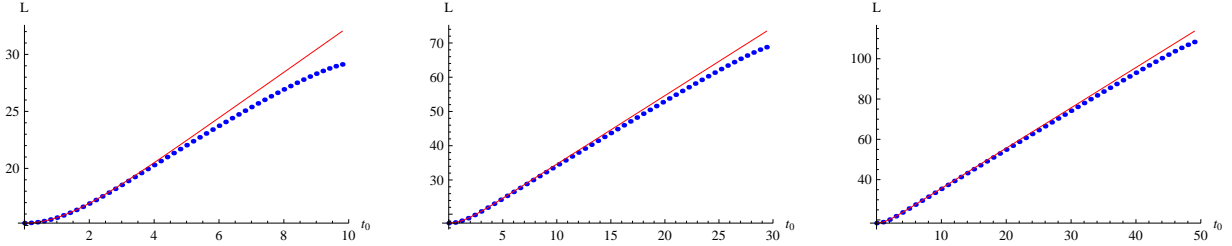


FIG. 1: Compare the geodesic length  $L(l, t_0)$  with analytical and semi-analytical formula, which are expressed using the red lines and blue points, respectively. The left, middle and right panels use the boundary separations  $l = 20, 60, 100$ , respectively. The UV cutoff has been set as  $r_0 = 100$ .

$t_0 r_H$  (Hereafter, we will set  $r_H = 1$  for convenience when we discuss the region of parameters sometimes and plot all the figures. But we keep it clear in all the formula.).

Note a simple but important observation from Eqs. (22), (23) and (24), that is, the implicit function  $s(l, t_0) \in [0, 1]$  and it decreases when  $l \rightarrow \infty$  or  $t_0/l \rightarrow 0$ . Thus, we can expand Eq. (23) as

$$l = \frac{4 \tanh\left(\frac{r_H t_0}{2}\right)}{r_H s} + \mathcal{O}(s)^1.$$

Immediately, one can have[70]

$$L(l, t_0) = 2 \ln \left[ l r_0 \cosh^2 \left( \frac{r_H t_0}{2} \right) \right]. \quad (27)$$

To see the effectiveness of Eq. (27), we compare it with the semi-analytical result of Eq. (26) in Fig. 1. One can find that they match well in a larger region of  $t_0$  when  $l \rightarrow \infty$ . Furthermore, the derivative of Eq. (27) is

$$\frac{dL}{dt_0} = 2 r_H \tanh \left( \frac{r_H t_0}{2} \right), \quad (28)$$

which approaches a constant limit fast when  $t_0$  increases, see Fig. 2.

## B. d=3 CFTs

For other theories with  $d > 2$ , we will use numerical methods to solve two equations of motion Eq. (9) and Eq. (10) with boundary conditions Eq. (11) and Eq. (12). Here we fix two small parameters as  $v_0 = 0.01$  and  $z_0 = 0.01$ . In order to obtain the numerical solutions, it would be found that the precision and time of the computation increase fast

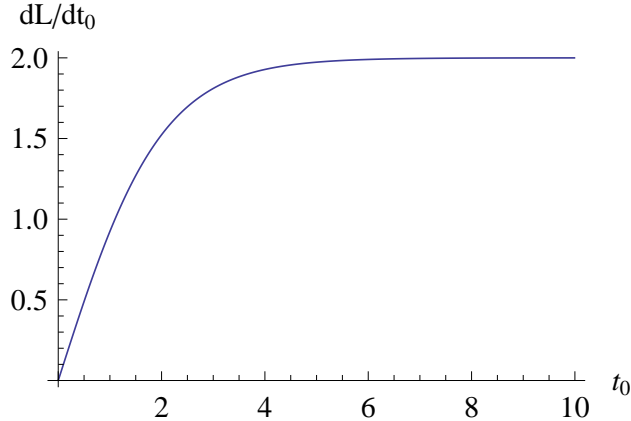


FIG. 2: The derivative of geodesic length  $L$  with respect to  $t_0$  as a function of  $t_0$ , using the analytical method.

when  $t_0$  and  $l$  increase. Fortunately, since we expect that the linear growth of HEE appears in the intermediate  $t_0$ , it is not necessary to solve the equations of motion in the region of very large  $t_0$ .

For  $d=3$  CFTs, substituting Eq. (2) into equations of motion and implementing a time-consumed computation with high precision, we can obtain  $z(y)$  and  $v(y)$  with fixed  $t_0$  and  $l$ . Consequently, we can integrate Eq. (7), which shows clearly that in the region of the intermediate  $t_0$  and large  $l$ , HEE grows linearly[71] and the growth rate approaches a constant when  $l$  increases, see Fig. 3. Note that we are comparing the HEE at any given time with the late time result  $S_{thermal}$ , which can be obtained from Eq. (14).

### C. Lifshitz gravity

Next we will consider the Lifshitz background, which can be regarded as the holographic dual to the non-relativistic scale-invariant (non-conformal) field theory. Solving the equations of motion with Eq. (4) and integrating Eq. (7), one can see the time evolution of HEE with different  $l$  in Fig. 4.

### D. GB gravity

In terms of Eq. (3) and Eq. (8), the similar behavior can be found in the HEE of field theories dual to 5-dim GB gravity, see Fig. 5.

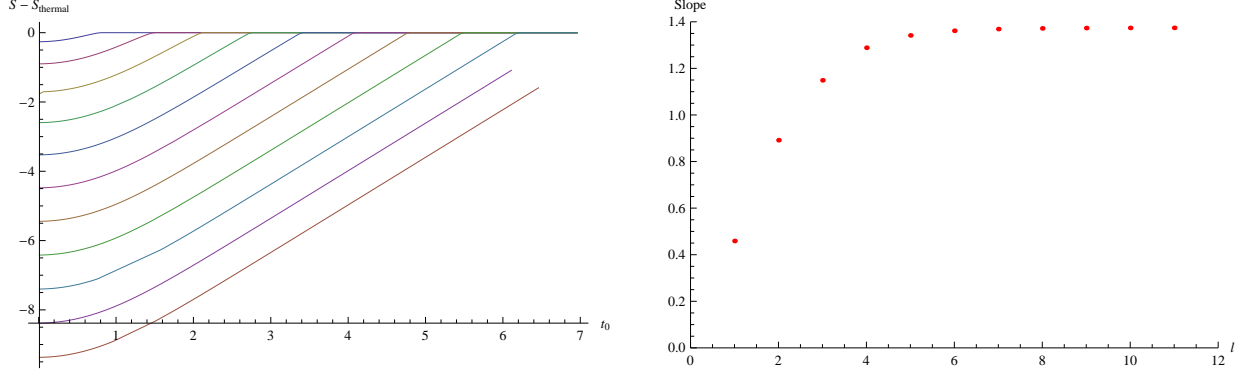


FIG. 3: Left:  $S - S_{\text{thermal}}$  for  $d=3$  CFTs as a function of  $t_0$  with different  $l$  from 1 (top) to 11 (down). Right: The derivative of HEE with respect to  $t_0$  at an intermediate value  $t_0 = l/2$ . The behaviour of the derivative will be not qualitatively changed if one selects other  $t_0$ , provided that it is not too small or too close to the thermalization time (that is what we mean by the “intermediate” time). We set  $4G_N^{d+1} = R^{d-2} = 1$  in all the figures for convenience.

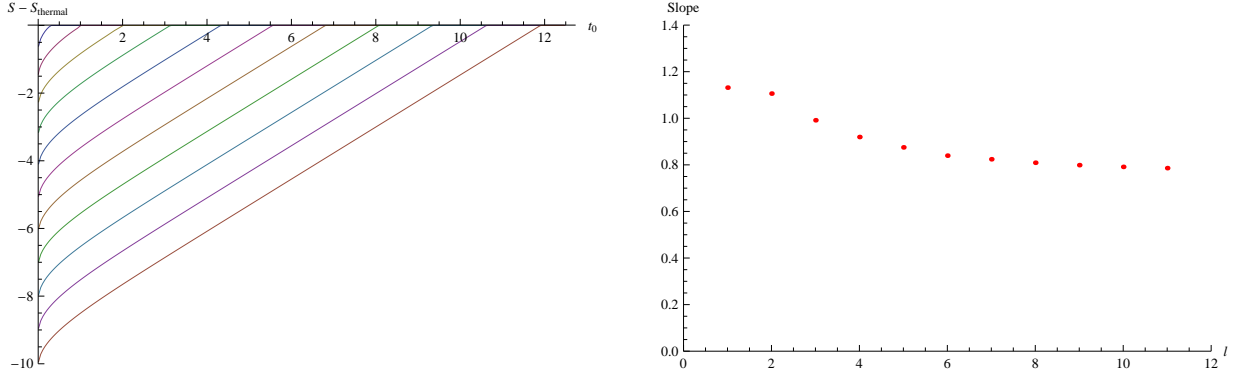


FIG. 4: Left:  $S - S_{\text{thermal}}$  for Lifshitz gravity as a function of  $t_0$  with different  $l$  from 1 (top) to 11 (down). Right: The derivative of HEE with respect to  $t_0$  at an intermediate value  $t_0 = l/4$ .

### III. LINEAR GROWTH OF HMI

By decomposing HEE and HMI [31, 32], Fischler et al. found that, when  $l \gg \beta$ , HMI contains the sub-leading area law of HEE in the static background. It was also shown that the decomposition of HEE and HMI is general for both  $d$ -dim relativistic CFTs and

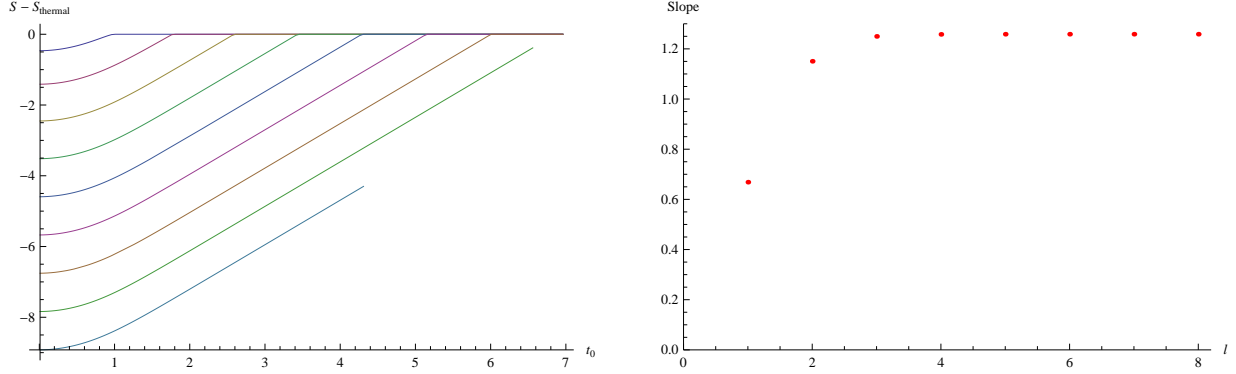


FIG. 5: Left:  $S - S_{\text{thermal}}$  for GB gravity as a function of  $t_0$  with different  $l$  from 1 (top) to 9 (down). Right: The derivative of HEE with respect to  $t_0$  at an intermediate value  $t_0 = 2l/3$ . We set  $\alpha = 0.05$  hereafter.

non-relativistic scale-invariant theories. In Appendix B, we prove that there is a similar decomposition in the holographic theories dual to GB gravity. Respecting the nontrivial correction of GB effect to the prescription of HEE, we believe that the decomposition is a very general result in strongly coupling field theories.

In this section, we will investigate the dynamical behavior of HMI, focusing on the region of large  $l$ . Our aim is to prove that the dynamical HMI at large  $l$  also can capture the behavior of the linear time growth with the  $l$ -independent rate of dynamical HEE that was shown in the above section. Let us introduce the prescription of HMI. Consider two disjoint rectangular subregion  $A$  and  $B$ . We set that they are same with one dimension of length  $l$  and are separated with distance  $x$ . HMI is defined by HEE as

$$I(A, B) = S_A + S_B - S_{A \cup B}.$$

For  $x \neq 0$ , there may be three choices of extremal surfaces which are anchored on the boundary of  $A \cup B$  [28]. But since in all the holographic theories we have shown that the HEE is monotonically increasing with respect to  $l$ , it is enough to consider HMI as

$$I(A, B) = 2S(l, t_0) - \min[2S(l, t_0), S(2l + x, t_0) + S(x, t_0)], \quad (29)$$

where  $S(l, t_0)$  denotes the HEE on the region  $A$  (or  $B$ ).

## A. d=2 CFTs

### 1. Analytical method for HMI with small $x$

Here we will study the HMI with large  $l$  based on the analytical expression of HEE Eq. (27). Obviously, Eq. (27) is not applicable to compute the HMI with general  $x$ . But fortunately, we can compute it for large  $l$ , intermediate  $t_0$  and small  $x$ . This is because the troubled term  $S(x, t_0)$  in Eq. (29) achieves the equilibrium value when  $t_0 > x/2$  [35] and can be replaced with the static one

$$S(x) = \frac{1}{2G_N^3} \ln \left[ \frac{2r_0 \sinh \left( \frac{r_H l}{2} \right)}{r_H} \right].$$

Thus, for  $x \ll \beta \ll l$ , Eq. (29) reads as

$$\begin{aligned} I &= 2S(l, t_0) - \min[2S(l, t_0), S(2l + x, t_0) + S(x)] \\ &= \frac{1}{2G_N^3} \ln \left[ \frac{l}{2x} \cosh^2 \left( \frac{r_H t_0}{2} \right) \right] + \mathcal{O}\left(\frac{x}{l}\right) + \mathcal{O}(x r_H)^2. \end{aligned}$$

Note that  $S(2l + x, t_0) + S(x)$  is smaller than  $2S(l, t_0)$  when  $x$  is so small. Comparing the dominated term with Eq. (27), one can find that HMI contains the exact time-dependent part of HEE in the region of small  $x$ .

### 2. Semi-analytical method for HMI with general $x$

Using the semi-analytical method, we can study HMI in the complete region of all the parameters, see Fig. 6[72]. In this figure, we will not care about the region with  $t_0 > l/2$  and  $t_0 > x/2$ , where  $S(l, t_0)$  and  $S(x, t_0)$  have achieved the equilibrium and HMI trivially reflects the dynamical behavior of  $S(2l + x, t_0)$ . Instead, we focus on the region with  $t_0 < l/2$ . One can find that the slope of the linear growth of HMI approaches a constant as  $l$  increases. To compare the slope of HMI and HEE, we plot in Fig. 7 the derivative of HMI and HEE with respect to  $t_0$  at an intermediate value of  $t_0 = l/4$  during the linear growth period. From this figure, one can find that the linear growth rate of HMI with different  $x$  approaches the rate of HEE when  $l$  increases. The effect of increasing  $x$  only enlarges the vanishing region of the growth rate of HMI at small  $l$  but the nonvanishing part at large  $l$  is nearly independent with  $x$ . Thus, we have shown that HMI can capture the behavior of the linear growth of the HEE with the  $l$ -independent rate even for general  $x$ .

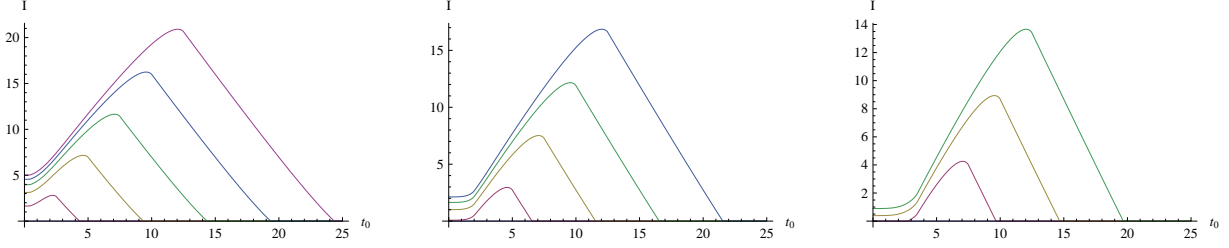


FIG. 6: HMI for d=2 CFTs as a function of  $t_0$ , using the semi-analytical method. From top to down, the boundary separations were taken as  $l = 25, 20, 15, 10, 5, 2$ . But HMI vanishes for  $l = 2$  in the left panel with  $x = 1$ , for  $l = 2, 5$  in the middle panel with  $x = 4$ , and for  $l = 2, 5, 10$  in the right panel with  $x = 7$ .

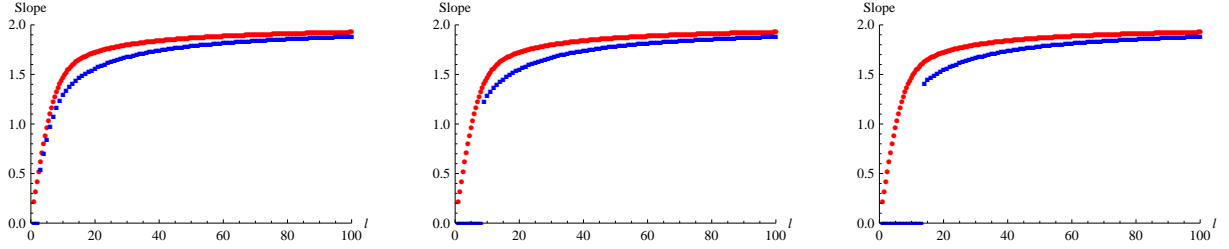


FIG. 7: The growth rate of HEE (red points) for d=2 CFTs and HMI (blue points) at  $t_0 = l/4$  as a function of  $l$  and  $x = 1, 4, 7$  for left, middle and right panels. The nonvanishing part of blue points at large  $l$  is nearly independent with  $x$ .

## B. Other holographic theories

Using the numerical method, we study the HMI in different theories. From Fig. 8 to Fig. 10, one can find that the linear time growth and the constant rate of dynamical HEE are presented in HMI for all the cases.



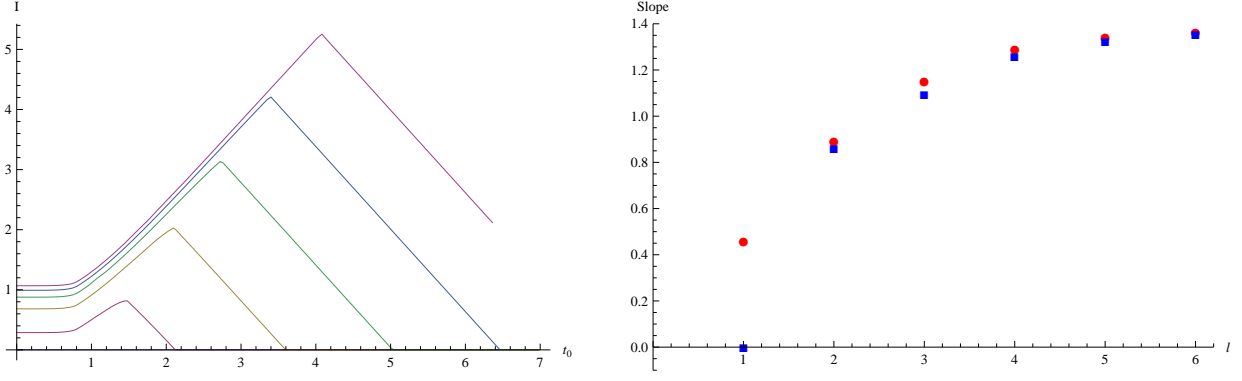


FIG. 8: (Left) HMI for  $d=3$  CFTs as a function of  $t_0$ . The boundary separations were taken as  $l = 6$  (top) to 1 (down). HMI vanishes for  $l = 1$ . (Right) The growth rate of HEE (red points) and HMI (blue points) at  $t_0 = l/2$  as a function of  $l$ . We set  $x = 1$ .

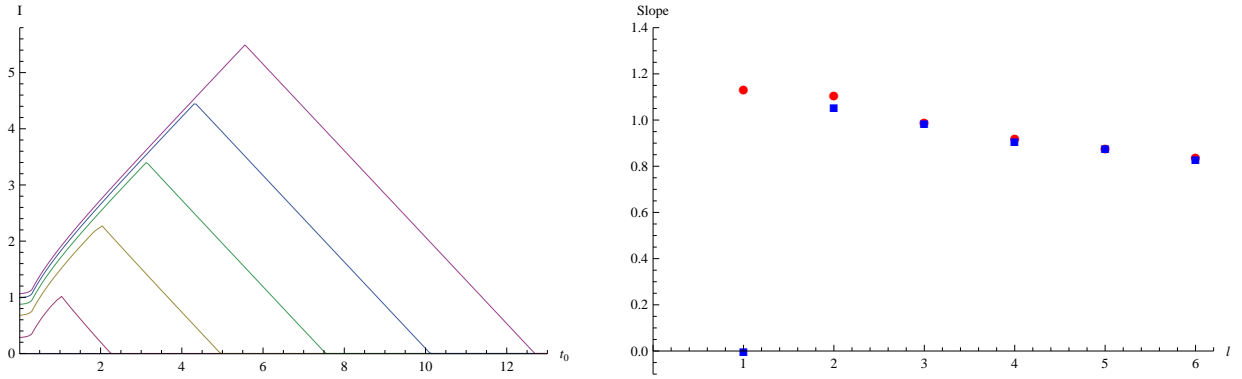


FIG. 9: (Left) HMI for Lifshitz gravity as a function of  $t_0$ . The boundary separations were taken as  $l = 6$  (top) to 1 (down). HMI vanishes for  $l = 1$ . (Right) The growth rate of HEE (red points) and HMI (blue points) at  $t_0 = l/4$  as a function of  $l$ . We set  $x = 1$ .

#### IV. LINEAR GROWTH OF HEE FROM THE INTERIOR OF APPARENT HORIZONS

Motivated by Hartman and Maldacena’s work [19], we will study the relationship between the linear growth of HEE in Vaidya models and the extension of the extremal surface in the interior of the apparent horizon (Note that by “interior”, it means the region between

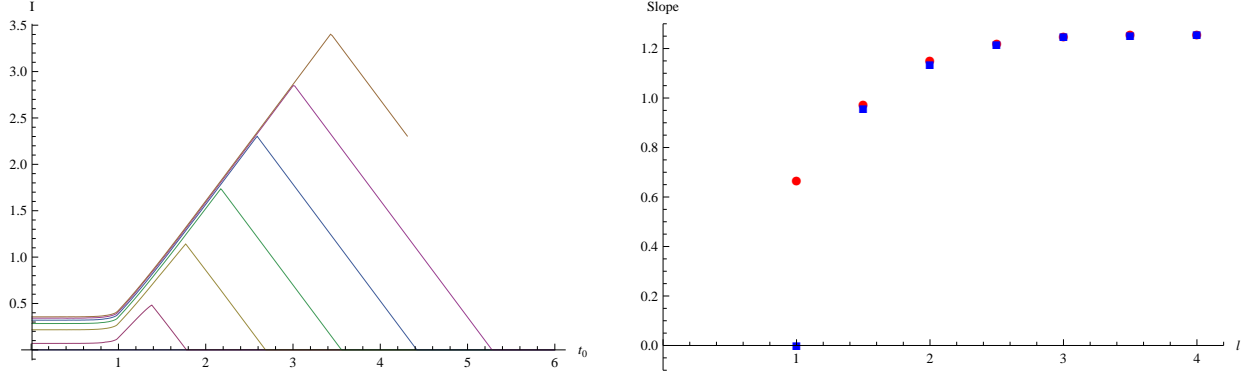


FIG. 10: (Left) HMI for GB gravity as a function of  $t_0$ . The boundary separations were taken as  $l = 4, 3.5, 3, 2.5, 2, 2.5, 1$  from top to down. HMI vanishes for  $l = 1$ . (Right) The growth rate of HEE (red points) and HMI (blue points) at  $t_0 = 2l/3$  as a function of  $l$ . We set  $x = 1$ .

the location of the apparent horizon and the singularity). Let us introduce the apparent horizon. It is sometimes called as marginal surfaces, defined as the boundary of trapped surfaces associated to a given foliation [57]. Thus, its location can be determined by one vanishing null expansion. In terms of the general metric (1), the tangent vector of ingoing and outgoing radial null geodesics can be read as

$$N^{in} = \frac{z^2}{f_2(z)} \partial_z, \quad N^{out} = \partial_v - \frac{1}{2z^{2n-2}} \frac{f_1(z, v)}{f_2(z)} \partial_z, \quad (30)$$

where we have used the normalization  $N^{in} \cdot N^{out} = -1$ . The expansion along outgoing null geodesics is given by

$$\theta = P^{\mu\nu} \nabla_\mu N_v^{out} \quad (31)$$

with the projective tensor

$$P_{\mu\nu} = g_{\mu\nu} + N_\mu^{in} N_v^{out} + N_v^{in} N_\mu^{out}.$$

Using Eqs. (1), (30) and (31) we have

$$\theta = \frac{d-1}{2z^{2n-1}} \frac{f_1(z, v)}{f_2(z)}.$$

Thus, for the holographic theories that we are interested in, the location of apparent horizons  $r_A(v)$  is determined by  $f_1(z, v) = 0$ .

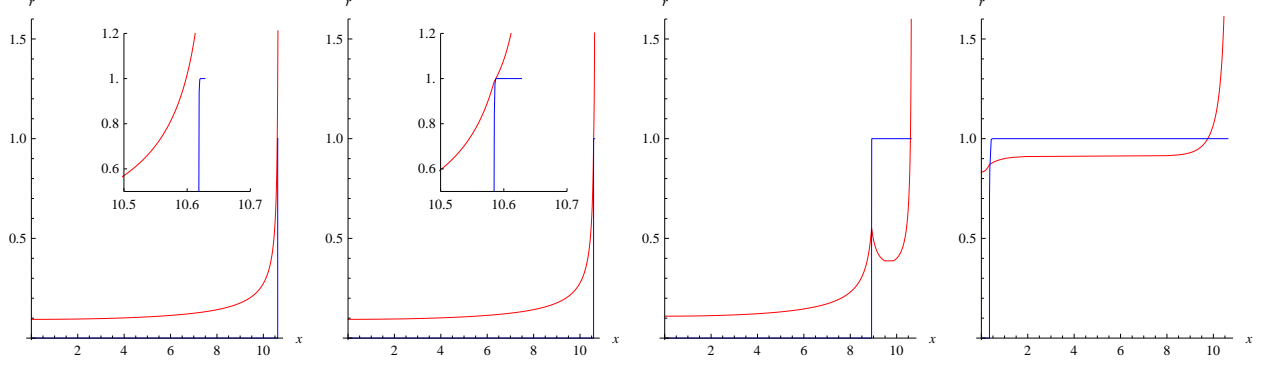


FIG. 11: Four typical relation between geodesics (red) and apparent horizons (blue) in the  $(x, r)$  plane.  $l$  is fixed as 21.3. From left to right,  $t_0 = 0.8, 1.12, 4, 10.6$ .

### A. $d=2$ CFTs

#### 1. Analytical method for the geodesic inside the horizon

Now we will use the analytical description of the geodesic in Sec. II. A to isolate the part of HEE contributed by the geodesic in the interior of apparent horizons. For this aim, let us plot some typical geodesics and apparent horizons using Eqs. (16), (17), (19) and (20), see Fig. 11. From these curves, one can extract three facts. First, it is possible that the geodesic crosses the apparent horizon twice. One crosspoint  $p$  is located at  $r_p = r_H$  and the other  $q$  at  $r_q = r_{sw}$ . Note that the location of crosspoint  $q$  can be understood since  $r_A(v)$  is a step function vanishing at  $v < 0$  and the nonvanishing radial location of crosspoints in Fig. 11 except  $r_p = r_H$  should be located at the position with  $v(r_{sw}) = 0$ . Second, when a geodesic crosses the apparent horizon, the branch 1 may crosses the horizon twice (see the rightmost panel in Fig. 11) or the branch 1 crosses at  $r_p = r_H$  and the branch 2 crosses at  $r_q = r_{sw}$  (see the third panel from left in Fig. 11). But as we have mentioned below Eq. (26), it is not necessary to consider both cases in the calculation since  $\lambda_+^{out}(r_{sw})$  with  $r_{sw} \geq r_H/\sqrt{2}$  has the same form as  $\lambda_-^{out}(r_{sw})$  with  $r_{sw} \leq r_H/\sqrt{2}$ . Third, the geodesic does not cross the apparent horizon when  $r_{sw} > r_H$ . With these facts in mind, we can write the length of the geodesic between two crosspoints as

$$L_{interior}(l, t_0) = 2 [\lambda_+^{out}(r_H) - \lambda_-^{out}(r_{sw})], \text{ with } r_{sw}(l, t_0) < r_H$$

$$= \ln \left[ \frac{4r_{sw}^4 (r_H^2 - r_*^2) + 4r_H^3 r_{sw}^2 \sqrt{r_{sw}^2 - r_*^2} + r_H^4 (r_{sw}^2 - r_*^2)}{r_H^4 (r_{sw}^2 - r_*^2) - 4r_H^2 r_{sw}^3 \left( r_{sw} + \sqrt{r_{sw}^2 - r_*^2} \right) - 4r_{sw}^4 \left[ r_*^2 - 2r_{sw} \left( r_{sw} + \sqrt{r_{sw}^2 - r_*^2} \right) \right]} \right], \quad (32)$$

where we have used the outside solutions of geodesic Eq. (15) and neglected the clear expression of restriction  $r_{sw}(l, t_0) < r_H$  hereafter for convenience. In terms of Eq. (24), we expand Eq. (32) with respect to  $s$

$$L_{interior}(l, t_0) = 2 \ln \left[ \frac{e^{r_H t_0} - 1}{2} \right] + \mathcal{O}(s)^2. \quad (33)$$

The derivative of its dominated term is

$$\frac{dL_{interior}}{dt_0} = \frac{2r_H}{1 - e^{-r_H t_0}}. \quad (34)$$

From Eq. (33) and Eq. (34), it is explicit that the length  $L_{interior}$  grows linearly and the slope approaches the constant  $2r_H$  fast when  $t_0$  increases, which is exactly same as the behavior of HEE seen in Eq. (27) and Eq. (28). To be more clear, we also compute the difference between Eq. (27) and Eq. (33)

$$L(l, t_0) - L_{interior}(l, t_0) = 2 \ln \left[ \frac{lr_0 e^{-r_H t_0} (1 + e^{r_H t_0})^2}{2(e^{r_H t_0} - 1)} \right],$$

which is close to the constant  $2 \log(lr_0/2)$  when  $t_0$  increases. Thus, we have proven analytically that the linear growth of HEE in the region of large  $l$  and intermediate  $t_0$  completely comes from the growth of geodesic length inside the apparent horizon.

## 2. Semi-analytical method for the geodesic inside the horizon

Based on Eq. (32) and the numerical solution of the implicit function  $s(l, t_0)$ , we can plot  $L_{interior}(l, t_0)$  in the complete region of parameters, see Fig. 12. One can find that the length  $L_{interior}$  grows linearly and its difference with  $L$  approaches a constant in the region of large  $l$  and intermediate  $t_0$ . The result is consistent with the analytical method, as it should be.

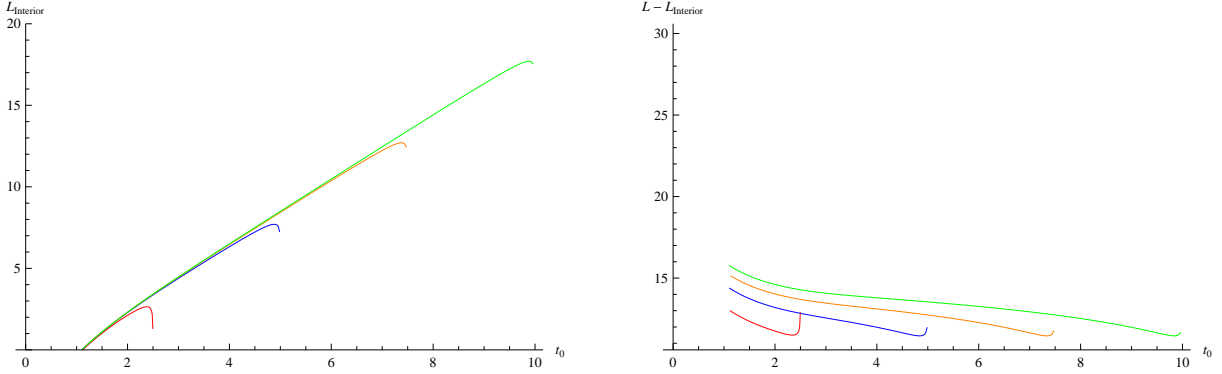


FIG. 12:  $L_{\text{interior}}$  (left) and  $L - L_{\text{interior}}$  (right) for  $d=2$  CFTs as functions of  $l$  and  $t_0$ . The boundary separations were taken to be  $l = 5, 10, 15, 20$  (red, blue, orange, green).

### B. Other holographic theories

For other theories with  $d > 2$ , we will resort to numerical methods. Solving the coordinates  $y_p$  and  $y_q$  of crosspoints  $p$  and  $q$  from

$$r_A[v(y)] = \frac{1}{z(y)}$$

and integrating Eq. (7) and Eq. (8) in the region within  $y \in [y_p, y_q]$ , one can obtain the contribution of the HEE from the extremal surface inside the apparent horizon, see Fig. 13, Fig. 14 and Fig. 15.

It is clear that the linear growth of HEE in these holographic theories all comes from the extension of the extremal surfaces in the interior of apparent horizons.

## V. CONCLUSION AND DISCUSSION

In this paper, using the gauge/gravity duality and Vaidya models, we investigated the thermalization process in strongly coupling field theories following a fast and homogeneous energy injection. We detected the holographic thermalization in terms of the HEE and focused on its behavior with the sufficiently large boundary separation. We studied various holographic theories, including the  $d=2$ ,  $d=3$  CFTs, the non-relativistic scale-invariant theory, and the dual theory of Gauss-Bonnet gravity. We obtained three *universal* results.

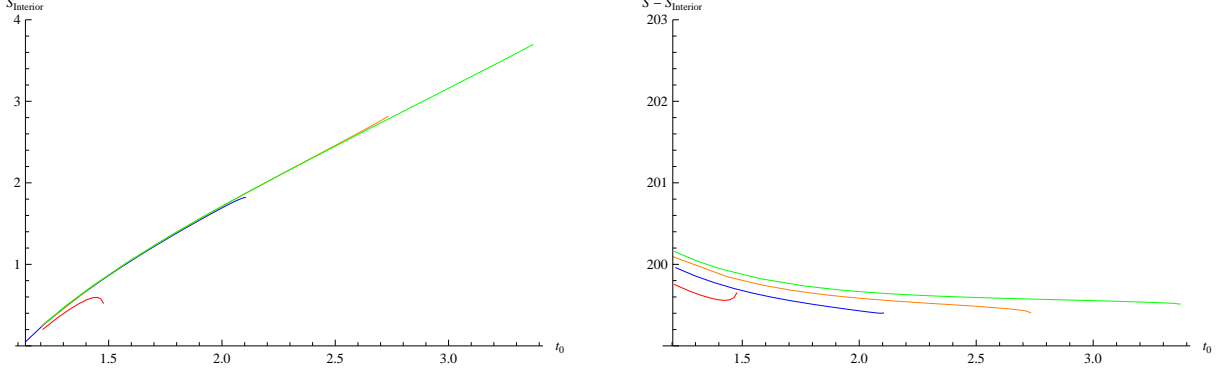


FIG. 13:  $S_{\text{interior}}$  (left) and  $S - S_{\text{interior}}$  (right) for d=3 CFTs as functions of  $l$  and  $t_0$ . The boundary separations were taken to be  $l = 2, 3, 4, 5$  (red, blue, orange, green).

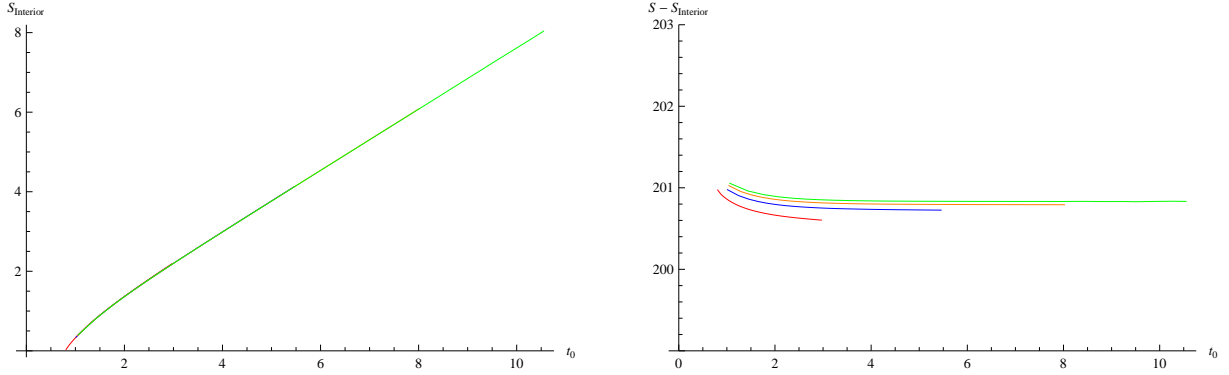


FIG. 14:  $S_{\text{interior}}$  (left) and  $S - S_{\text{interior}}$  (right) for Lifshitz gravity as functions of  $l$  and  $t_0$ . The boundary separations were taken to be  $l = 4, 6, 8, 10$  (red, blue, orange, green). Note that for different  $l$  their  $S_{\text{interior}}$  grows almost along the same curve.

First, for large spatial scale  $l$ , the evolution of HEE includes an intermediate stage during which it grows linearly and the growth rate approaches a  $l$ -independent constant when the scale increases. Second, the time-dependent HMI captures the behavior of the linear growth with the  $l$ -independent rate exactly. Third, the linear growth of HEE at large  $l$  is related to the interior of the apparent horizon along the extremal surface. In particular, all the results are obtained analytically for d=2.

Besides the three main results, we would like to point out an interesting phenomenon

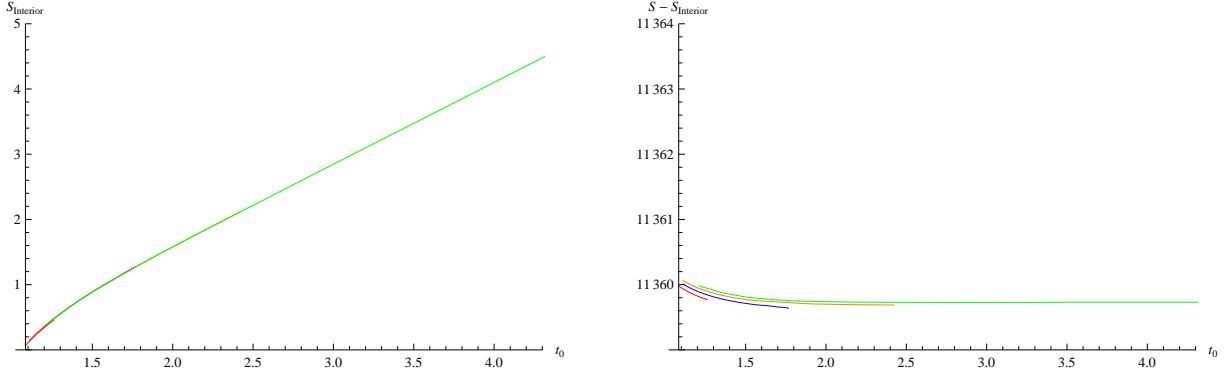


FIG. 15:  $S_{\text{interior}}$  (left) and  $S - S_{\text{interior}}$  (right) for GB gravity as functions of  $l$  and  $t_0$ . The boundary separations were taken to be  $l = 1.5, 2, 3, 7$  (red, blue, orange, green).

that the growth rate of HEE in the Lifshitz theory initially decreases with respect to  $t_0$ , which is different with all the other theories.

We also found that the interior of the event horizon can capture the linear growth of HEE, see Appendix C. However, it was observed that the extremal surface inside the event horizon involves the extra part in the vacuum, which has nothing to do with the behavior of the linear growth. Thus, we argue that the apparent horizon seems to capture the linear growth behavior of HEE more exactly than the event horizon does.

At last, we note that the time-dependent HEE can be schematically decomposed as

$$S = S_{EH} + S_{BB} = S_{AH} + S_{VAC} + S_{BB}$$

where  $S_{AH}$ ,  $S_{EH}$ ,  $S_{BB}$  and  $S_{VAC}$  denote the partial HEE contributed by the extremal surface inside apparent horizons, event horizons, black branes and vacuum, respectively. Such kind of decomposition suggests that some observables on the boundary have a natural structure determined by the nontrivial locations in the bulk. It is interesting to study in the future whether the identification of the structure could be significant in the dual field theories.

Note added: After we finished this paper, we noticed a recent preprint [63], in which Liu and Suh have obtained analytically the universal scaling of the HEE in Vaidya models by studying the geometry around and inside the event horizon.

## Acknowledgments

SFW would like to thank Hong Liu for very helpful discussion on the local nature of entanglement propagation. SFW and YQW were supported by National Natural Science Foundation of China (No. 11275120 and No. 11005054).

## Appendix A: The Vaidya metric for Lifshitz gravity

The 4-dim infalling shell geometry in asymptotically Lifshitz background described by the Vaidya metric in Poincaré coordinates will be given in this section. The authors of Ref. [55] have obtained a static black hole solution in four dimensions that asymptotically approaches the Lifshitz spacetime in a system with a strongly-coupled scalar. The action is

$$S = \frac{1}{2} \int d^4x \sqrt{-g} (R - 2\Lambda) - \int d^4x \sqrt{-g} \left( \frac{e^{-2\varphi}}{4} F^2 + \frac{m^2}{2} A^2 + e^{-2\varphi} - 1 \right)$$

where  $\Lambda = -\frac{n^2+(d-2)n+(d-1)^2}{2}$  is the cosmological constant and  $m^2 = (d-1)n$ . The solution of this system is:

$$ds^2 = -f \frac{dt^2}{z^{2n}} + \frac{d\vec{x}^2}{z^2} + \frac{dz^2}{fz^2}, \quad A = \frac{f}{\sqrt{2}z^2} dt, \quad \varphi = -\frac{1}{2} \log(1 + z^2/z_H^2), \quad (\text{A1})$$

with  $f = 1 - Mz^2$  and  $n = 2$ . Using the coordinate transformation

$$dt = dv + \frac{z^{n-1}}{f} dz,$$

the metric in Eq. (A1) will become

$$ds^2 = -z^{2n}(1 - Mz^2)dv^2 - 2z^{-1-n}dzdv + z^{-2}d\vec{x}^2.$$

Consider Einstein's and Maxwell's equations

$$T_{\mu\nu} = R_{\mu\nu} - \frac{1}{2}Rg_{\mu\nu} + \Lambda g_{\mu\nu} - e^{-2\varphi} F_\mu^\gamma F_{\nu\gamma} - m^2 A_\mu A_\nu + g_{\mu\nu} \left( \frac{e^{-2\varphi}}{4} F^2 + \frac{m^2}{2} A^2 + e^{-2\varphi} - 1 \right) \quad (\text{A2})$$

$$J^\nu = e^{-2\varphi} \nabla_\mu F^{\mu\nu} - m^2 A^\nu. \quad (\text{A3})$$

We find that there exists a Vaidya solution with the form

$$\begin{aligned} ds^2 &= -z^{2n} [1 - m(v)z^2] dv^2 - 2z^{-1-n} dzdv + z^{-2} d\vec{x}^2, \\ A_\mu &= \frac{1 - m(v)z^2}{\sqrt{2}z^2} \delta_\mu^v + \frac{z^{n-1}}{\sqrt{2}z^2} \delta_\mu^r, \\ \varphi(v, z) &= -\frac{1}{2} \log[1 + m(v)z^2], \end{aligned}$$



that means, the only nonvanishing components of Eq. (A2) and Eq. (A3) are given by

$$T_{vv} = m'(v), \quad J_v = \sqrt{2}z^2 m'(v).$$

One can see that the only difference between the dynamic solution and the static one is to replace the mass parameter  $M$  with a mass function  $m(v)$ .

## Appendix B: Decomposition of static HEE and HMI by numerical methods

In Ref. [31], it is interesting to see that the static HEE (both for  $d$ -dim relativistic CFTs and non-relativistic scale-invariant theories) at high temperature (i.e.  $l \gg \beta$ ) can be analytically decomposed as  $S = S_{div} + S_{thermal} + S_{finite} + S_{corr}$ . Moreover, for  $l \gg \beta$  and  $x \ll \beta$ , HMI can be decomposed as  $I = I_{div} + S_{finite} + I_{corr}$  [32]. Now we would like to study whether there is a similar decomposition in the field theory dual to GB gravity. However, it seems difficult to analytically calculate HEE in the GB background since its prescription is nontrivially corrected, see Eq. (6). Fortunately, we can achieve the decomposition by numerical fitting.

At the beginning, let us review the analytical decomposition for  $d$ -dim CFTs and illustrate the effectiveness of our numerical methods in d=4 CFTs. It has been found that Eq. (14) with  $l \gg \beta$  can be decomposed analytically as

$$S \simeq S_{div} + \frac{(r_H R)^{d-2}}{4G_N^{d+1}} (kr_H l + \mathcal{S}_{high} - \mathcal{E}_1 e^{-\mathcal{E}_0 r_H l}). \quad (\text{B1})$$

The divergent term can be gotten by computing Eq. (14) in the pure  $AdS$  spacetime where  $M = 0$ , which gives rise to  $S_{div} = \frac{R^{d-2}}{4G_N^{d+1}} \frac{2}{(d-2)z_0^{d-2}}$ . The constant  $k = 1$  and  $\mathcal{E}_0 = \sqrt{d(d-1)/2}$ . The constants  $\mathcal{S}_{high}$  and  $\mathcal{E}_1$  are made of many gamma functions [31]. For our aim, we calculate them for d=4, which are

$$\mathcal{S}_{high} = -0.665925, \quad \mathcal{E}_1 = 1.437285. \quad (\text{B2})$$

Moreover, the HEE (14) at low temperature (i.e.  $l \ll \beta$ ) can be analytically expanded as

$$S \simeq S_{div} + \frac{R^{d-2}}{4G_N^{d+1}} \frac{\mathcal{S}_0}{l^{d-2}} \left[ 1 + \mathcal{S}_1 (r_H l)^d \right]. \quad (\text{B3})$$

When d=4,

$$\mathcal{S}_0 = -0.320664, \quad \mathcal{S}_1 = -1.763956. \quad (\text{B4})$$

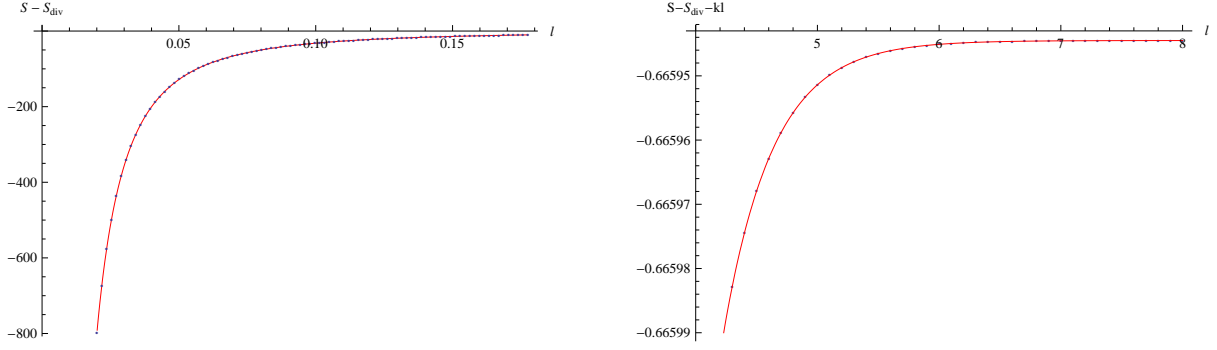


FIG. 16: Fitting the HEE for  $d=4$  CFTs at small (left) and large (right)  $l$ . The blue points are the data of HEE and the red lines are our fitting functions.

Combing Eq. (B1) and Eq. (B3), one can decompose the HMI to

$$I \simeq \frac{(r_H R)^{d-2}}{4G_N^{d+1}} \left[ \frac{-\mathcal{S}_0}{(r_H x)^{d-2}} + \mathcal{S}_{high} - k r_H x - \mathcal{S}_0 \mathcal{S}_1 (r_H x)^2 \right],$$

when  $l \gg \beta$  and  $x \ll \beta$ .

Now we invoke the numerical methods. By numerically fitting Eq. (B1) and Eq. (B3) with Eq. (14) in the region with large and small  $l$ , respectively, we extract the constants

$$\mathcal{S}_{high} = -0.665944, \quad \mathcal{E}_1 = 1.439163.$$

$$\mathcal{S}_0 = -0.320664, \quad \mathcal{S}_1 = -1.763732,$$

which match Eq. (B2) and Eq. (B4) very well, see Fig. 16.

We go further to study the GB gravity. The divergent term of the static HEE can be calculated as  $S_{div} = \frac{R^2}{4G_N^5} \frac{2\alpha + L_c^2}{z_0^2 L_c^3}$ . Fitting the HEE with Eq. (B1) and Eq. (B3) in different region of  $l$ , see Fig. 17, we find that the constants  $k$  and  $\mathcal{E}_0$  should be equal to the rescaled values

$$k(\alpha) = -\frac{1}{L_c^3}, \quad \mathcal{E}_0(\alpha) = -\sqrt{\frac{d(d-1)}{2}} \frac{1}{L_c}.$$

The remained constants can be obtained for different  $\alpha$ . For instance, when  $\alpha = 0.05$ ,

$$\mathcal{S}_{high}(\alpha) = -0.845791, \quad \mathcal{S}_0(\alpha) = -0.401275, \quad \mathcal{S}_1(\alpha) = -1.276055.$$

Hereto, we have shown that the decomposition of static HEE at low and high temperature has the general form for  $d$ -dim CFTs and the field theory dual to GB gravity. Consequently, the decomposition of HMI is general too.

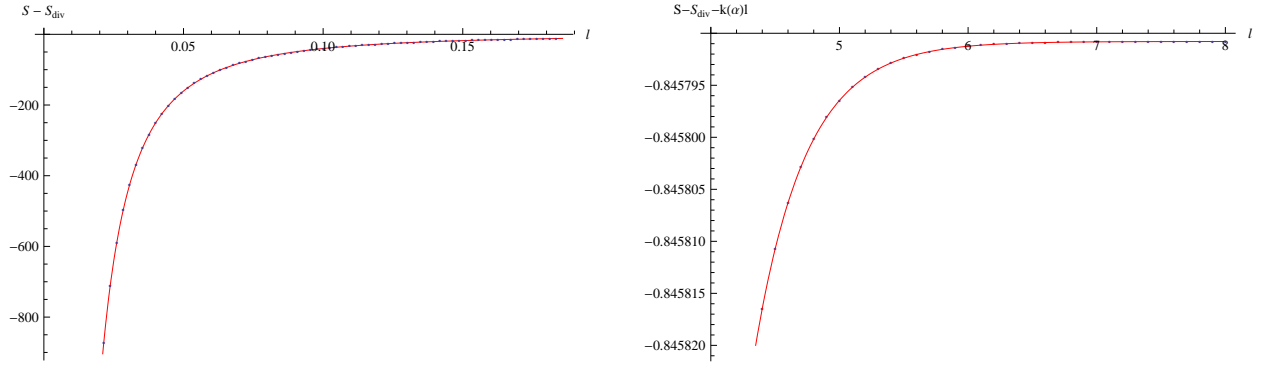


FIG. 17: Fitting the HEE for the GB gravity at small (left) and large (right)  $l$ . The blue points are the data of HEE and the red lines are our fitting functions.

### Appendix C: Linear growth of HEE from the interior of event horizons

Here we would like to study whether the event horizon can also capture the behavior of the linear growth of HEE. The event horizon is a null hypersurface generated by outgoing null geodesics. According to the general metric (1), its location can be determined by a differential equation

$$f_1[z(v), v] + 2z(v)^{2n-2} f_2[z(v)] \frac{dz(v)}{dv} = 0$$

with the boundary condition of connecting the apparent horizon in the future of  $v = 0$  [62]. By numerical computations, we find that when the extremal surface intersects the apparent horizon, the event horizon always lie outside the extremal surface, see Fig. 18 for instance. Thus, in such cases, one can evaluate the part of the HEE contributed by the extremal surface inside the event horizon by subtracting the part in the pure black brane from the whole HEE. In the following, we will show that the subtracted part is independent with  $t_0$  in the region with large  $l$  and intermediate  $t_0$ . Since we have demonstrated that the contribution of the extremal surface involving both the vacuum and the pure black brane are independent with  $t_0$ , we can conclude that the part of HEE contributed by the extremal surface inside the event horizon grows linearly as the behavior of complete HEE.

Let us consider  $d=2$  CFTs that can be described analytically. The length of the desired

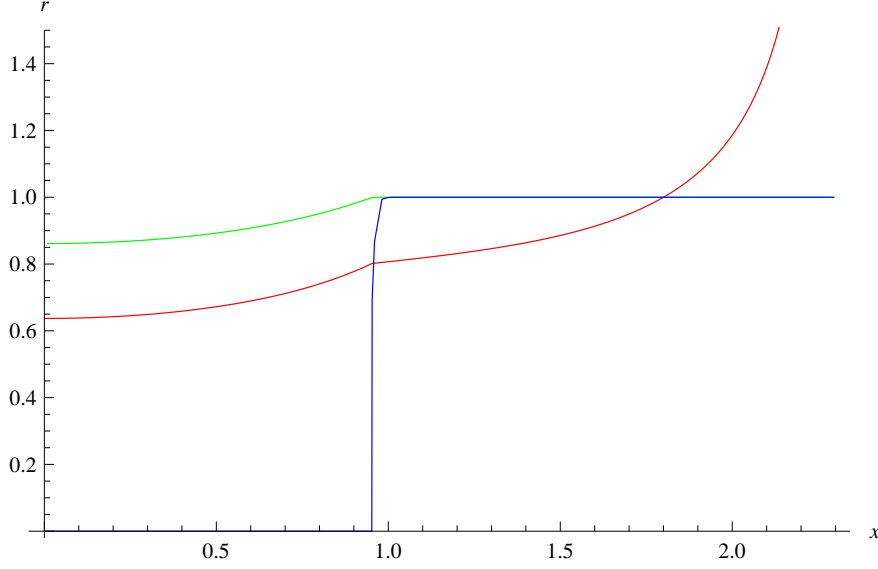


FIG. 18: The geodesic line (red), the apparent horizon (blue) and the event horizon (green) as a function of  $x$  for fixed  $t_0 = 2$  and  $l = 4.6$  in d=2 CFTs.

geodesic outside the event horizon (i.e. the geodesic in the pure black brane) is

$$\begin{aligned} L_{outside}(l, t_0) &= 2 [\lambda_+^{out}(r_0) - \lambda_+^{out}(r_H)] \\ &= 2 \ln \left( \frac{2r_0}{r_H} \right) - \ln \left( 1 - \frac{r_s^2}{r_H^2} + \frac{r_H \sqrt{r_{sw}^2 - r_s^2}}{r_{sw}^2} + \frac{r_H^2 (r_{sw}^2 - r_s^2)}{4r_{sw}^4} \right). \end{aligned}$$

When  $s$  is small, the length can be expanded as

$$L_{outside}(l, t_0) = 2 \ln \left( \frac{r_0}{r_H} \right) + 2 \ln (1 + e^{r_H t_0}) - 2r_H t_0 + \mathcal{O}(s)^2.$$

Obviously, it approaches a constant  $2 \log (r_0/r_H)$  when  $t_0$  increases.

We numerically plot Fig. 19 that reveals the constant contribution to the HEE from the extremal surface in the pure black branes for various holographic theories.

- 
- [1] J. M. Maldacena, *The Large N Limit of Superconformal Field Theories and Supergravity*, *Adv. Theor. Math. Phys.* **2** (1998) 231 [hep-th/9711200]; S. S. Gubser, I. R. Klebanov, A. M. Polyakov, *Gauge Theory Correlators from Non-Critical String Theory*, *Phys. Lett. B* **428** (1998) 105 [hep-th/9802109]; E. Witten, *Anti De Sitter Space And Holography*, *Adv. Theor. Math. Phys.* **2** (1998) 253 [hep-th/9802150].

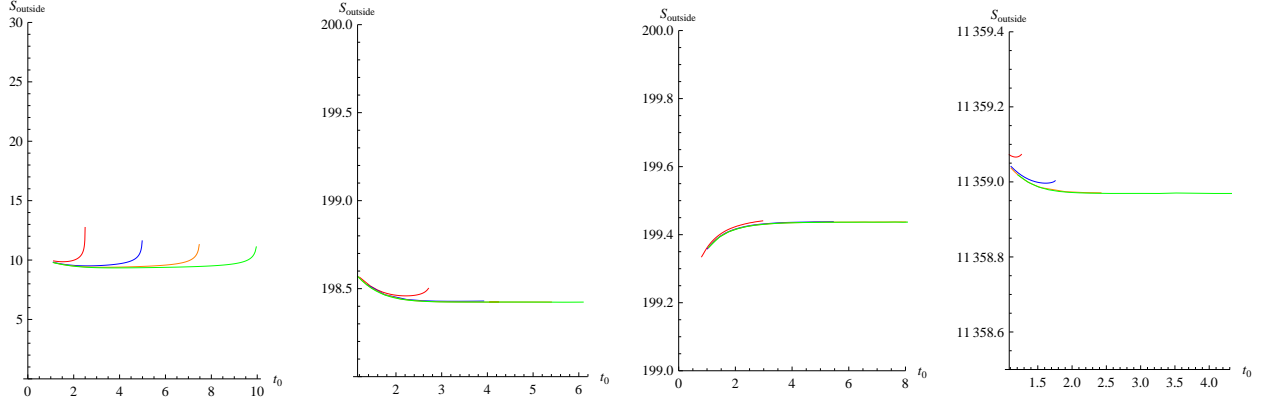


FIG. 19: The constant contribution to the HEE from the extremal surfaces in the pure black branes for various holographic theories. From left to right, they are d=2 CFTs ( $l = 5, 10, 15, 20$ ), d=3 CFTs ( $l = 2, 3, 4, 5$ ), Lifshitz gravity ( $l = 4, 6, 8, 10$ ) and GB gravity ( $l = 1.5, 2, 3, 7$ ). In each panel the red, blue, orange and green lines represent different  $l$  from small to large.

- [2] See following reviews: F. Gelis, *The early stages of a high energy heavy ion collision*, *J. Phys. Conf. Ser.* **381** (2012) 012021 [arXiv:1110.1544]; B. Müller and A. Schäfer, *Entropy creation in relativistic heavy ion collisions*, arXiv:1110.2378; E. Iancu, *QCD in heavy ion collisions*, arXiv:1205.0579.
- [3] R. Baier, A. H. Mueller, D. Schi and D. T. Son, *Bottom-up thermalization in heavy ion collisions*, *Phys. Lett. B* **502** (2001) 51 [hep-ph/0009237]; A. H. Mueller, A. I. Shoshi and S. M. H. Wong, *A Possible Modified "bottom-up" Thermalization in Heavy Ion Collisions*, *Phys. Lett. B* **632** (2006) 257 [hep-ph/0505164].
- [4] See following reviews: S. Mondal, D. Sen and K. Sengupta, *Non-equilibrium dynamics of quantum systems: order parameter evolution, defect generation, and qubit transfer*, arXiv:0908.2922; J. Dziarmaga, *Dynamics of a quantum phase transition and relaxation to a steady state*, arXiv:0912.4034; A. Polkovnikov, K. Sengupta, A. Silva and M. Vengalattore, *Nonequilibrium dynamics of closed interacting quantum systems*, *Rev. Mod. Phys.* **83** (2011) 863 [arXiv:1007.5331].
- [5] M. A. Nielsen and I. L. Chuang, *Quantum computation and quantum information*, Cambridge University Press, 2000.
- [6] P. Calabrese and J. L. Cardy, *Entanglement entropy and quantum field theory*, *J. Stat. Mech.*

- 0406** (2004) P06002 [hep-th/0405152]; A. Kitaev and J. Preskill, *Topological entanglement entropy*, *Phys. Rev. Lett.* **96** (2006) 110404 [hep-th/0510092]; M. Levin and X. G. Wen, *Detecting Topological Order in a Ground State Wave Function*, *Phys. Rev. Lett.* **96** (2006) 110405 [cond-mat/0510613]; B. Hsu, M. Mulligan, E. Fradkin and E. A. Kim, *Universal entanglement entropy in 2D conformal quantum critical points*, *Phys. Rev. B* **79** (2009) 115421 [arXiv:0812.0203].
- [7] S. Ryu and T. Takayanagi, *Holographic Derivation of Entanglement Entropy from AdS/CFT*, *Phys. Rev. Lett.* **96** (2006) 181602 [hep-th/0603001]; S. Ryu and T. Takayanagi, *Aspects of holographics entanglement entropy*, *JHEP* **08** (2006) 045 [hep-th/0605073].
- [8] See a recent review: T. Takayanagi, *Entanglement Entropy from a Holographic Viewpoint*, *Class. Quant. Grav.* **29** (2012) 153001 [arXiv:1204.2450].
- [9] A. Lewkowycz and J. Maldacena, *Generalized gravitational entropy*, arXiv:1304.4926.
- [10] M. Van Raamsdonk, *Comments on quantum gravity and entanglement*, arXiv:0907.2939; M. Van Raamsdonk, *Building up spacetime with quantum entanglement*, *Gen. Rel. Grav.* **42** (2010) 2323 [arXiv:1005.3035].
- [11] H. Casini, M. Huerta and R. C. Myers, *Towards a derivation of holographic entanglement entropy*, *JHEP* **05** (2011) 036 [arXiv:1102.0440]; E. Bianchi and R. C. Myers, *On the Architecture of Spacetime Geometry*, arXiv:1212.5183.
- [12] V. E. Hubeny and M. Rangamani, *Causal Holographic Information*, arXiv:1204.1698;
- [13] V. E. Hubeny, M. Rangamani, E. Tonni, *Thermalization of Causal Holographic Information*, arXiv:1302.0853.
- [14] B. Swingle, *Entanglement Renormalization and Holography*, *Phys. Rev. D* **86** (2012) 065007 [arXiv:0905.1317]; *Constructing holographic spacetimes using entanglement renormalization*, arXiv:1209.3304.
- [15] J. Molina-Vilaplana and P. Sodano, *Holographic View on Quantum Correlations and Mutual Information between Disjoint Blocks of a Quantum Critical System*, *JHEP* **10** (2011) 011 [arXiv:1108.1277].
- [16] V. Balasubramanian, M. B. McDermott and M. Van Raamsdonk, *Momentum-space entanglement and renormalization in quantum field theory*, arXiv:1108.3568; H. Matsueda, *Scaling of entanglement entropy and hyperbolic geometry*, arXiv:1112.5566; M. Ishihara, F. L. Lin and B. Ning, *Refined Holographic Entanglement Entropy for the AdS Solitons and AdS black Holes*,

- arXiv:1203.6153; H. Matsueda, M. Ishihara and Y. Hashizume, *Tensor Network and Black Hole*, arXiv:1208.0206.
- [17] M. Nozaki, S. Ryu and T. Takayanagi, *Holographic Geometry of Entanglement Renormalization in Quantum Field Theories*, *JHEP* **10** (2012) 193 [arXiv:1208.3469].
  - [18] M. Nozaki, T. Numasawa and T. Takayanagi, *Holographic Local Quenches and Entanglement Density*, arXiv:1302.5703.
  - [19] T. Hartman and J. Maldacena, *Time Evolution of Entanglement Entropy from Black Hole Interiors*, arXiv:1303.1080.
  - [20] G. Vidal, *Entanglement renormalization*, *Phys. Rev. Lett.* **99** (2007) 220405 [cond-mat/0512165]; G. Vidal, *Entanglement renormalization: an introduction*, arXiv:0912.1651; J. Haegeman, T. J. Osborne, H. Verschelde and F. Verstraete, *Entanglement renormalization for quantum fields*, *Phys. Rev. Lett.* **110** (2013) 100402 [arXiv:1102.5524]; G. Evenbly and G. Vidal, *Quantum Criticality with the Multi-scale Entanglement Renormalization Ansatz*, arXiv:1109.5334.
  - [21] V. E. Hubeny, M. Rangamani and T. Takayanagi, *A Covariant Holographic Entanglement Entropy Proposal*, *JHEP* **07** (2007) 062 [arXiv:0705.0016].
  - [22] M. M. Wolf, F. Verstraete, M. B. Hastings, and J. I. Cirac, *Area laws in quantum systems: Mutual information and correlations*, *Phys. Rev. Lett.* **100** (2008) 070502 [arXiv:0704.3906].
  - [23] B. Swingle, *Mutual information and the structure of entanglement in quantum field theory*, arXiv:1010.4038.
  - [24] S. Furukawa, V. Pasquier and J. Shiraishi, *Mutual Information and Boson Radius in  $c=1$  Critical Systems in One Dimension*, *Phys. Rev. Lett.* **102** (2009) 170602 [arXiv:0809.5113]; P. Calabrese, J. Cardy and E. Tonni, *Entanglement entropy of two disjoint intervals in conformal field theory*, *J. Stat. Mech.* (2009) P11001 [arXiv:0905.2069 [hep-th]]; P. Calabrese, J. Cardy and E. Tonni, *Entanglement entropy of two disjoint intervals in conformal field theory II*, *J. Stat. Mech.* **1101** (2011) P01021 [arXiv:1011.5482].
  - [25] M. Headrick, *Entanglement Renyi entropies in holographic theories*, *Phys. Rev. D* **82** (2010) 126010 [arXiv:1006.0047].
  - [26] V. E. Hubeny and M. Rangamani, *Holographic entanglement entropy for disconnected regions*, *JHEP* **03** (2008) 006 [arXiv:0711.4118].
  - [27] E. Tonni, *Holographic entanglement entropy: near horizon geometry and disconnected regions*,

- JHEP* **05** (2011) 004 [arXiv:1011.0166].
- [28] V. Balasubramanian, A. Bernamonti, N. Copland, B. Craps and F. Galli, *Thermalization of mutual and tripartite information in strongly coupled two dimensional conformal field theories*, *Phys. Rev. D* **84** (2011) 105017 [arXiv:1110.0488].
  - [29] A. Allais and E. Tonni, *Holographic evolution of the mutual information*, *JHEP* **01** (2012) 102 [arXiv:1110.1607].
  - [30] R. Callan, J. He, and M. Headrick, *Strong subadditivity and the covariant holographic entanglement entropy formula*, *JHEP* **06** (2012) 081 [arXiv:1204.2309].
  - [31] W. Fischler and S. Kundu, *Strongly Coupled Gauge Theories: High and Low Temperature Behavior of Non-local Observables*, arXiv:1212.2643.
  - [32] W. Fischler, A. Kundu and S. Kundu, *Holographic Mutual Information at Finite Temperature*, arXiv:1212.4764.
  - [33] S. Bhattacharyya and S. Minwalla, *Weak Field Black Hole Formation in Asymptotically AdS Spacetimes*, *JHEP* **09** (2009) 034 [arXiv:0904.0464].
  - [34] S. R. Das, T. Nishioka and T. Takayanagi, *Probe Branes, Time-dependent Couplings and Thermalization in AdS/CFT*, *JHEP* **07** (2010) 071 [arXiv:1005.3348]; H. Ebrahim and M. Headrick, *Instantaneous Thermalization in Holographic Plasmas*, BRX-TH 624 [arXiv:1010.5443]; D. Garfinkle and L. A. Pando Zayas, *Rapid Thermalization in Field Theory from Gravitational Collapse*, *Phys. Rev. D* **84** (2011) 066006 [arXiv:1106.2339]; S. R. Das, *Holographic Quantum Quench*, *J. Phys. Conf. Ser.* **343** (2012) 012027 [arXiv:1111.7275]; A. Buchel, L. Lehner and R. C. Myers, *Thermal quenches in  $\mathcal{N} = 2^*$  plasmas*, *JHEP* **08** (2012) 049 [arXiv:1206.6785]; X. Gao, A. M. Garcia-Garcia, H. B. Zeng and H. Q. Zhang, *Lack of thermalization in holographic superconductivity*, arXiv:1212.1049; W. H. Baron, D. Galante and M. Schvellinger, *Dynamics of holographic thermalization*, *JHEP* **03** (2013) 070 [arXiv:1212.5234].
  - [35] J. Abajo-Arrastia, J. Aparicio and E. Lopez, *Holographic Evolution of Entanglement Entropy*, *JHEP* **11** (2010) 149 [arXiv:1006.4090].
  - [36] J. Aparicio and E. Lopez, *Evolution of Two-Point Functions from Holography*, *JHEP* **12** (2011) 082 [arXiv:1109.3571].
  - [37] T. Albash and C. V. Johnson, *Evolution of Holographic Entanglement Entropy after Thermal and Electromagnetic Quenches*, *New J. Phys.* **13** (2011) 045017 [arXiv:1008.3027].
  - [38] V. Balasubramanian, A. Bernamonti, J. de Boer, N. Copland, B. Craps, E. Keski-Vakkuri, B.



- Müller and A. Schäfer, *Thermalization of Strongly Coupled Field Theories*, *Phys. Rev. Lett.* **106** (2011) 191601 [arXiv:1012.4753]; V. Balasubramanian, A. Bernamonti, J. de Boer, N. Copland, B. Craps, E. Keski-Vakkuri, B. Müller and A. Schäfer, *Holographic Thermalization*, *Phys. Rev. D* **84** (2011) 026010 [arXiv:1103.2683].
- [39] V. Keranen, E. Keski-Vakkuri, L. Thorlacius, *Thermalization and entanglement following a non-relativistic holographic quench*, *Phys. Rev. D* **85** (2012) 026005 [arXiv:1110.5035].
- [40] D. Galante and M. Schvellinger, *Thermalization with a chemical potential from AdS spaces*, *JHEP* **07** (2012) 096 [arXiv:1205.1548]; E. Caceres and A. Kundu, *Holographic Thermalization with Chemical Potential*, *JHEP* **09** (2012) 055 [arXiv:1205.2354]; E. Caceres, A. Kundu, J. F. Pedrazab, W. Tangarife, *Strong Subadditivity, Null Energy Condition and Charged Black Holes*, arXiv:1304.3398.
- [41] X. X. Zeng and W. B. Liu, *Holographic thermalization in Gauss-Bonnet gravity*, arXiv:1305.4841.
- [42] S. Lin and E. Shuryak, *Toward the AdS/CFT Gravity Dual for High Energy Collisions.3. Gravitationally Collapsing Shell and Quasiequilibrium*, *Phys. Rev. D* **78** (2008) 125018 [arXiv:0808.0910].
- [43] P. Calabrese and J. Cardy, *Evolution of Entanglement Entropy in One-dim Systems*, *J. Stat. Mech.* **0504** (2005) P04010 [cond-mat/0503393].
- [44] P. Calabrese and J. Cardy, *Quantum Quenches in Extended Systems*, *J. Stat. Mech.* **0706** (2007) P06008 [arXiv:0704.1880].
- [45] P. Billingsley, *Ergodic Theory and Information*, Wiley, New York, 1965; V. Latora and M. Baranger, *Kolmogorov-Sinai Entropy Rate versus Physical Entropy*, *Phys. Rev. Lett* **82** (1999) 520 [chao-dyn/9806006].
- [46] J. Bolte, B. Müller, and A. Schäfer, *Ergodic properties of classical SU(2) lattice gauge theory*, *Phys. Rev. D* **61** (2000) 054506 [hep-lat/9906037]; T. Kunihiro et al., *Chaotic behavior in classical Yang-Mills dynamics*, *Phys. Rev. D* **82** (2010) 114015 [arXiv:1008.1156].
- [47] D. V. Fursaev, *Proof of the holographic formula for entanglement entropy*, *JHEP* **0609** (2006) 018 [arXiv:hep-th/0606184].
- [48] J. de Boer, M. Kulaxizi, A. Parnachev, *Holographic Entanglement Entropy in Lovelock Gravities*, *JHEP* **04** (2011) 025 [arXiv:1101.5781].
- [49] L. Y. Hung, R. C. Myers and M. Smolkin, *On Holographic Entanglement Entropy and Higher*

- Curvature Gravity*, *JHEP* **04** (2011) 025 [arXiv:1101.5813].
- [50] See the recent proof of EE proposal in GB gravity: A. Bhattacharyya, A. Kaviraj and A. Sinha, *Entanglement entropy in higher derivative holography*, arXiv:1305.6694.
  - [51] C. T. Asplund and S. G. Avery, *Evolution of Entanglement Entropy in the D1-D5 Brane System*, *Phys. Rev. D* **84** (2011) 124053 [arXiv:1108.2510].
  - [52] P. Basu and S. R. Das, *Quantum Quench across a Holographic Critical Point*, *JHEP* **01** (2012) 103 [arXiv:1109.3909].
  - [53] A. Buchel, L. Lehner, R. C. Myers and A. van Niekerk, *Quantum quenches of holographic plasmas*, arXiv:1302.2924.
  - [54] T. Kobayashi, *A Vaidya-type radiating solution in Einstein-Gauss-Bonnet gravity and its application to braneworld*, *Gen. Rel. Grav.* **37** (2005) 1869 [gr-qc/0504027]; H. Maeda, *Effects of Gauss-Bonnet term on the final fate of gravitational collapse*, *Class. Quant. Grav.* **23** (2006) 2155 [gr-qc/0504028]; A. E. Dominguez and E. Gallo, *Radiating black hole solutions in Einstein-Gauss-Bonnet gravity*, *Phys. Rev. D* **73** (2006) 064018 [gr-qc/0512150].
  - [55] K. Balasubramanian and J. McGreevy, *An analytic Lifshitz black hole*, *Phys. Rev. D* **80** (2009) 104039 [arXiv:0909.0263].
  - [56] S. N. Solodukhin, *Entanglement Entropy in Non-Relativistic Field Theories*, *JHEP* **04** (2010) 101 [arXiv:0909.0277]; D. Nesterov and S. N. Solodukhin, *Gravitational effective action and entanglement entropy in UV modified theories with and without Lorentz symmetry*, *Nucl. Phys. B* **842** (2011) 141 [arXiv:1007.1246].
  - [57] S. W. Hawking and G. F. R. Ellis, *The Large scale structure of space-time*, Cambridge University Press, Cambridge, 1973.
  - [58] P. M. Chesler and L. G. Yaffe, *Horizon formation and far-from-equilibrium isotropization in supersymmetric Yang-Mills plasma*, *Phys. Rev. Lett.* **102** (2009) 211601 [arXiv:0812.2053]; P. M. Chesler and L. G. Yaffe, *Boost invariant flow, black hole formation, and far-from-equilibrium dynamics in  $N = 4$  supersymmetric Yang-Mills theory*, *Phys. Rev. D* **82** (2010) 026006 [arXiv:0906.4426].
  - [59] P. Figueras, V. E. Hubeny, M. Rangamani and S. F. Ross, *Dynamical black holes and expanding plasmas*, *JHEP* **04** (2009) 137 [arXiv:0902.4696].
  - [60] T. Takayanagi and T. Ugajin, *Measuring Black Hole Formations by Entanglement Entropy via Coarse-Graining*, *JHEP* **11** (2010) 054 [arXiv:1008.3439].

- [61] J. D. Brown and M. Henneaux, *Central Charges In The Canonical Realization Of Asymptotic Symmetries: an example from three dimensional gravity*, *Commun. Math. Phys.* 104 (1986) 207.
- [62] E. Poisson, *A Relativist's Toolkit*, Cambridge University Press, 2004.
- [63] H. Liu and S. J. Suh, *Entanglement Tsunami: Universal Scaling in Holographic Thermalization*, arXiv:1305.7244.
- [64] In Ref. [32], it was argued that HMI is a better guide than HEE to capturing quantum entanglement.
- [65] In Ref. [38], the maximal growth rate is used to characterize the linear growth, since the linear regime covers the time at which the growth rate is maximal.
- [66] In this paper, we denote the numerical method as solving differential equations numerically and the semi-analytic method as solving some complicated algebra equations numerically.
- [67] It has been suggested that the apparent horizon may be more suitable than the event horizon as a notion of entropy in the holographic theory out of equilibrium [21, 58–60]. With this in mind, we prefer to demonstrate the relationship between apparent horizon and the linear growth of HEE. But we will also study the event horizon in the last of the paper.
- [68] We will denote them briefly as  $d$ -dim CFTs, Lifshitz gravity and GB gravity, respectively.
- [69] See other asymptotically-Lifshitz Vaidya spacetimes in [39].
- [70] After finishing this paper, we were kindly informed by E. Lopez that Eq. (27) has been obtained in [36].
- [71] For the holographic theories with  $d > 2$ , there would be two or three extremal surfaces when  $t_0$  increases. We have selected the one with the minimal HEE.
- [72] Note that the dynamical HMI in  $d = 2$  and  $d = 3$  CFTs have been studied in Refs. [28, 29], but they did not pay attention to the constant growth rate that appears in the region of large  $l$ .